

Article

Effects of Coating of Dicarboxylic Acids on the Mass#Mobility Relationship of Soot Particles

Huaxin Xue, Alexei F. Khalizov, Lin Wang, Jun Zheng, and Renyi Zhang

Environ. Sci. Technol., **2009**, 43 (8), 2787-2792 • DOI: 10.1021/es803287v • Publication Date (Web): 18 March 2009

Downloaded from <http://pubs.acs.org> on April 13, 2009

More About This Article

Additional resources and features associated with this article are available within the HTML version:

- Supporting Information
- Access to high resolution figures
- Links to articles and content related to this article
- Copyright permission to reproduce figures and/or text from this article

[View the Full Text HTML](#)



ACS Publications
High quality. High impact.

Environmental Science & Technology is published by the American Chemical Society, 1155 Sixteenth Street N.W., Washington, DC 20036

Effects of Coating of Dicarboxylic Acids on the Mass–Mobility Relationship of Soot Particles

HUAXIN XUE, ALEXEI F. KHALIZOV,
LIN WANG, JUN ZHENG, AND
RENYI ZHANG*

Department of Atmospheric Sciences and Department of
Chemistry, Texas A&M University,
College Station, Texas 77843

Received November 20, 2008. Revised manuscript received
January 28, 2009. Accepted February 16, 2009.

A tandem differential mobility analyzer (TDMA) and a differential mobility analyzer–aerosol particle mass analyzer (DMA-APM) have been employed to study morphology and hygroscopicity of soot aerosol internally mixed with dicarboxylic acids. The effective densities, fractal dimensions, and dynamic shape factors of soot particles before and after coating with succinic and glutaric acids are determined. Coating of soot with succinic acid results in a significant increase in the particle mobility diameter, mass, and effective density, but these properties recover to their initial values once succinic acid is removed by heating, suggesting that no restructuring of the soot core occurs. This conclusion is also supported from the observation of similar fractal dimensions and dynamic shape factors for fresh and coated/heated soot aggregates. Also, no change is observed when succinic acid-coated aggregates are cycled through elevated relative humidity (5% to 90% to 5% RH) below the succinic acid deliquescence point. When soot is coated with glutaric acid, the particle mass increases, but the mobility diameter shrinks by 10–40%. Cycling the soot aerosol coated with glutaric acid through elevated relative humidity leads to an additional mass increase, indicating that condensed water remains within the coating even at low RH. The fractal dimension of soot particles increases after coating and remains high when glutaric acid is removed by heating. The dynamic shape factor of glutaric acid-coated and heated soot is significantly lower than that of fresh soot, suggesting a significant restructuring of the soot agglomerates by glutaric acid. The results imply that internal mixing of soot aerosol during atmospheric aging leads to changes in hygroscopicity, morphology, and effective density, which likely modify their effects on direct and indirect climate forcing and deposition in the human respiratory system.

Introduction

Soot particles are ubiquitous in the troposphere and are of current interest because of their impacts on regional air quality and climate by altering cloud formation and radiation balance (1–3). Soot is produced by incomplete combustion of fossil fuels and biomass at a global emission rate of 8–24 Tg C yr⁻¹ (1). Freshly emitted soot particles are typically hydrophobic and unlikely to act as cloud condensation nuclei (CCN). However, chemical and physical aging during at-

mospheric transport considerably alters hygroscopicity, morphology, and composition of soot particles (4), resulting in stronger direct and indirect effects of soot on climate.

Soot particles are emitted as complex aggregates, and their structure is directly related to their atmospheric fate and deposition efficiency in the human respiratory system. The fractal dimension (D_f) is an indirect measure of the morphology of irregularly shaped agglomerated particles. It is defined and calculated in several different ways and varies in the range of 1 to 3, with 3 for compact spheres and 1 in the limit of infinitely long straight chain agglomerates (5). A technique, which uses simultaneous differential mobility analyzer (DMA) and aerosol particle mass analyzer (APM) measurements to determine the effective density and fractal dimension of gas-borne particles from the relationship between their electrical mobility diameter and mass, has been developed by McMurry and co-authors (6). The mass-fractal dimension, D_f , based on mobility diameter, d_{me} , and particle mass, m , is defined as:

$$m \propto d_{me}^{D_f} \quad (1)$$

The hydrophobic soot particles typically exhibit little structural or morphological differences between dry and saturated relative humidity (RH) conditions, whereas hydrophilic soot particles produced by condensation of water-soluble compounds such as H₂SO₄ and glutaric acid collapse into globules when relative humidity is increased (7, 8). The extent of restructuring depends on the origin of soot and also the mass fraction and type of the coating material. Carbon soot aggregates from spark discharge collapse to more compact structures at high RH, but diesel combustion particles exhibit only limited restructuring (9) because of the hydrophobic organic coating composed primarily of lubricating oil, unburned hydrocarbons, and PAHs (10).

Internal mixing of soot with glutaric acid transforms the particles from hydrophobic to hydrophilic state and modifies their morphology, enhancing their ability to absorb and scatter solar radiation (7). Thus, low-molecular weight dicarboxylic organic acids, representing a significant component of fine particulate matter in the troposphere (11), may enhance the climatic effects of soot aerosol. However, the physical properties of C3–C9 dicarboxylic acids exhibit a strong alternating trend with the number of the carbon atoms (12, 13), implying that the observations made for soot coated by glutaric acid may not be directly applied to other members of the dicarboxylic acid family and further experimental studies are required.

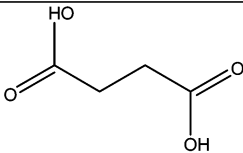
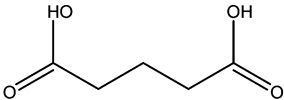
In this work we have studied the flame-generated soot aerosol particles coated by succinic and glutaric acids, representing dicarboxylic acids with even and odd numbers of carbon atoms, respectively (Table 1). The effect of coating on the mobility diameter and the mass of size-classified aerosol are measured by a combined tandem-DMA (TDMA) and DMA-APM techniques. The mobility-mass relationship allows determination of the effective density, fractal dimension, and dynamic shape factor of soot before and after soot processing, which includes coating with dicarboxylic organic acids, exposure to water vapor, drying, and heating.

Experimental Section

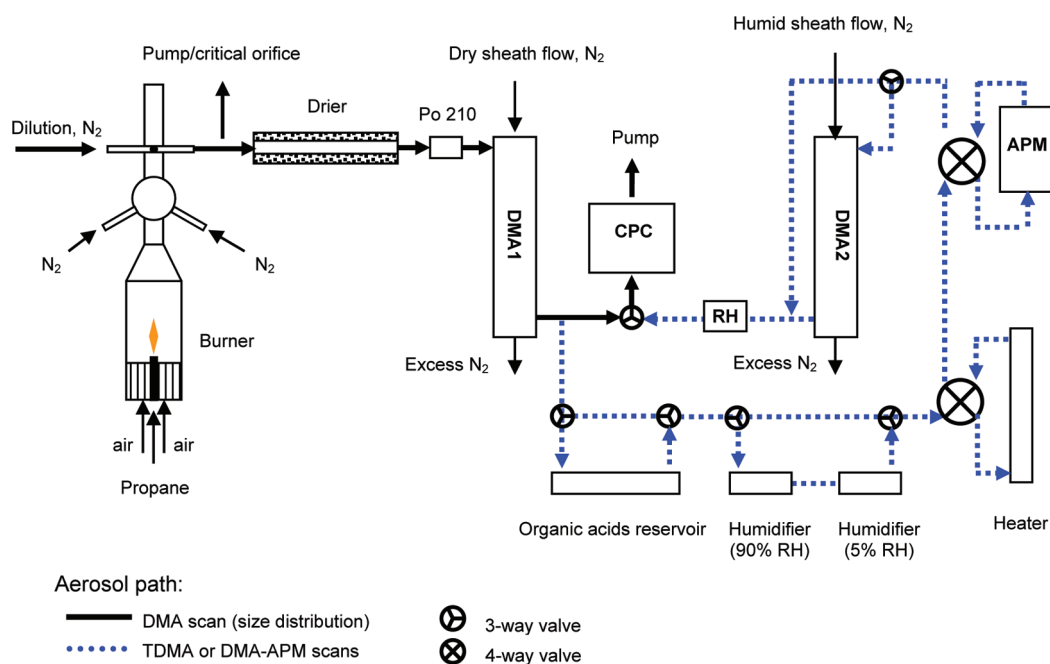
A schematic of the present experimental setup is shown in Figure 1. The fresh soot aerosol was passed through a Po-210 bipolar charger, mobility-classified with DMA1, and processed through a combination of coating, humidification,

* Corresponding author.

TABLE 1. Chemical Structures and Physical Properties of Succinic and Glutaric Acids

	Succinic acid	Glutaric acid
Structure		
Melting temperature, °C ^a	188	96
Vapor pressure at 25 °C, Pa ^a	3.9×10 ⁻⁵	6.7×10 ⁻⁴
Density at 25°C, g/cm ^a	1.57	1.42
Solubility at 25 °C, g/100 g H ₂ O ^b	8.8	116
Deliquescence RH, % ^b	>99	83-89

^a From ref 12. ^b From ref 13.


FIGURE 1. Schematic of the TDMA and DMA-APM system.

drying, and heating. The resulting changes in the particle mobility size and mass were quantified using DMA2 and APM, respectively. There were no observable changes in monodispersity of the particle size and mass distributions after processing.

Aerosol Generation and Sampling. Soot aerosol was generated in a laminar diffusion burner by combustion of propane (4, 8). The soot sampling system consisted of a horizontally mounted stainless steel tube with a 1 mm orifice. Coagulation of the primary particles led to formation of submicron soot fractal aggregates with a geometric mean diameter of 130 nm and geometric standard deviation of 1.8. Two crossing dilution N₂ flows at the top of the burner provided uniform mixing and dilution of soot and prevented

further coagulation. Soot aerosol was diluted by a 7 LPM N₂ carrier gas flow and then passed through a diffusion drier and a Nafion drier to reduce the RH to below 1%. Polystyrene latex (PSL, Duke Scientific Inc.) aerosol employed as a reference in DMA-APM measurements of particle density was produced by nebulizing a suspension of the spheres in deionized water (17 MΩ) using an atomizer (Model 376001, TSI Inc.).

Aerosol Coating and Conditioning. Mobility-classified aerosol was introduced in a heated reservoir filled with a coating material, i.e., succinic or glutaric acid. The organic vapor was entrained into the aerosol flow, and condensed on particles upon cooling to room temperature. The concentrations of dicarboxylic acids in the coating reservoir were

estimated to be about 4×10^{13} molecule cm^{-3} for succinic acid and 9×10^{12} molecule cm^{-3} for glutaric acid using ion drift–chemical ionization spectrometry (ID-CIMS) (14–16). The residence time in the reservoir was about 20 s. To study the effect of relative humidity, coated soot aerosol was admitted through a humidifier maintained at 90% RH and then dried to ~5% RH. Additional experiments were performed by heating the processed soot aerosol to 200 °C to remove the organic coating.

Tandem DMA (TDMA). TDMA was employed to measure the mobility size change of soot aerosol particles upon processing. The diametric growth factor, Gfd, is defined as the ratio of coated soot mobility diameter measured by DMA2 to the fresh soot diameter selected by DMA1. Both DMAs (long DMA 3081, TSI Inc.) were operated at a sheath flow rate of 6.5 LPM N_2 and sample flow 1.0 LPM. The relative error in measured diametric growth factors was below 1%.

DMA-APM. The application of DMA-APM technique for mass–mobility measurements has been previously described in detail (6, 8). The mass of a particle that passed through the APM (APM-3600, Kanomax Inc., Japan) is determined by the rotational speed of cylindrical electrodes and voltage applied to the inner electrode (the outer electrode is grounded). Aerosol mass distribution was determined by stepping the voltage at a fixed rotation speed and measuring the concentration of particles passing through APM by CPC (Model 3760, TSI Inc.). Mass growth factor for coated particles, Gfm, is calculated according to

$$\text{Gfm} = \frac{m_{\text{coated}}}{m_{\text{fresh}}} = \frac{V_{\text{APM,coated}}}{V_{\text{APM,fresh}}} \quad (2)$$

where m_{fresh} and m_{coated} are the fresh and coated particle mass, and $V_{\text{APM,fresh}}$ and $V_{\text{APM,coated}}$ are the peak APM voltages corresponding to the peak masses for the mobility-selected fresh and coated particles. The effective density of fresh and coated soot particles, ρ_{eff} , is measured relative to the density of PSL particles according to

$$\rho_{\text{eff}} = \frac{V_{\text{APM,soot}}}{V_{\text{APM,PSL}}} \times \frac{\rho_{\text{PSL}}}{\text{Gfd}_{\text{soot}}} \quad (3)$$

where $V_{\text{APM, soot}}$ and $V_{\text{APM, PSL}}$ are the peak APM voltages corresponding to the peak masses for soot and PSL particles with identical initial mobility diameter, $\rho_{\text{PSL}} = 1.054 \text{ g cm}^{-3}$ is the material density of polystyrene latex, and Gfd_{soot} is the diametric growth factor for coated soot ($\text{Gfd}_{\text{soot}} = 1$ for fresh soot). The relative errors in measured mass growth factors and effective densities were below 4%.

Results and Discussion

Mass-Mobility Relationship. Succinic Acid. The mobility diameters of soot and PSL particles increase upon coating by succinic acid, and smaller particles exhibit larger growth as shown in Figure 2a. When coated soot particles are cycled through elevated RH (5–90–5% RH), their mobility diameter decreases by 2–6%, with stronger shrinking for larger particles. Subsequent heating of these particles to remove succinic acid results in growth factors ranging from 0.95 to 0.97. Without humidification, heating the coated soot aerosol leads to growth factors of 0.97–0.99. The observed shrinking of coated soot upon humidification is caused by partial restructuring of the soot cores and filling of the interstitial space between primary spheres by succinic acid aqueous solution formed at high RH. Even though succinic acid is expected to be solid below its deliquescence point (Table 1), several monolayers of water condensed on the hydrophilic acid surface apparently lead to a minor compaction of the coated aggregates.

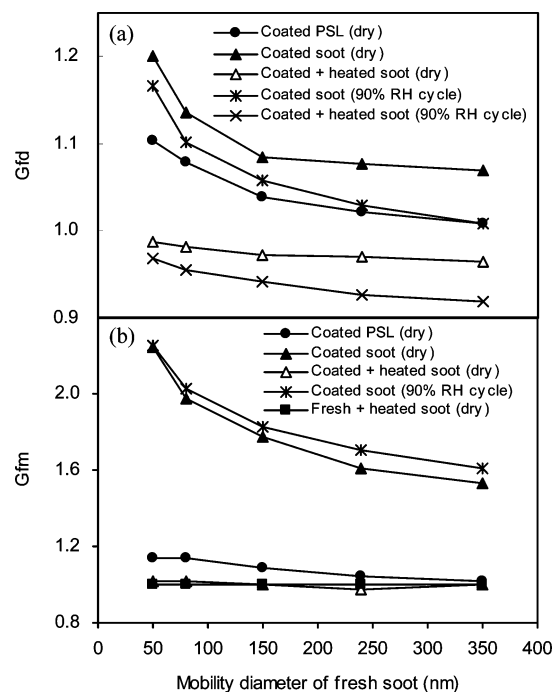


FIGURE 2. Mobility diameter (a) and mass (b) growth factors of soot and PSL particles upon coating by succinic acid. Measurements were performed using mobility-classified aerosol with initial diameters of 50, 80, 150, 240, and 350 nm.

For spherical particles, such as PSL, the diametric growth factor provides an indication of the coating volume fraction. In the case of soot aggregates, however, the condensed material can be distributed between the primary spheres of the aggregate, and the change in the mobility diameter may have a complex relation with the actual coating mass. Our DMA-APM measurements show that the coated soot particles contain 35–55% succinic acid by mass with the corresponding mass growth factors ranging from 1.53 to 2.24 (Figure 2b). The lower mass growth for particles with larger initial size is in agreement with the trend observed for sulfuric acid-coated soot (8). When the coated soot is passed through the heater, the mass ratio of coated to fresh soot is reduced to 1.00 ± 0.05 , illustrating that condensed succinic acid is completely removed. The mass growth factor of uncoated heated soot is 0.99 ± 0.05 , indicating that the fraction of volatile materials at 200 °C, e.g., organic carbon, is negligible. The high RH cycle measurements show a small but reproducible mass increase of coated soot particles, indicating that a small amount of water vapor absorbed at 90% RH remains in the coating even after drying to 5% RH.

The effective density of fresh soot calculated from the mass–mobility relationship decreases with the increasing mobility size (Figure 3). Once coated with organic acid, the aggregates become denser, but the effective density remains significantly lower than the inherent bulk density of soot or succinic acid. The fractal dimension determined using eq 1 shows a small variation between fresh ($D_f = 2.20$) and coated ($D_f = 2.21$) soot. On the contrary, coated and heated soot has a slightly increased fractal dimension under both dry ($D_f = 2.29$) and high RH cycle ($D_f = 2.30$) conditions. The small restructuring of coated aggregates upon heating to 200 °C can be caused by the melted succinic acid (Table 1).

Glutaric Acid. The changes in mobility diameter of PSL and soot particles exposed to glutaric acid are presented in Figure 4a. The mobility diameter of soot aggregates decreases by 10–40% upon coating, suggesting that internal mixing with glutaric acid significantly alters the soot morphology. The shrinking effect is more significant for agglomerates with larger initial mobility size, which have lower effective density.

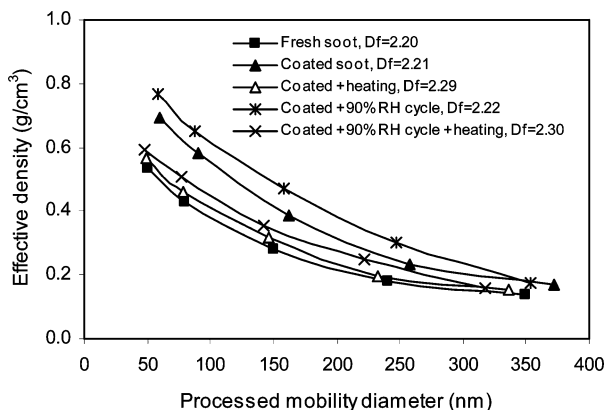


FIGURE 3. Effective densities of fresh and succinic acid-coated soot particles as a function of processed mobility diameter. The fractal dimension (D_f) was obtained using eq 1.

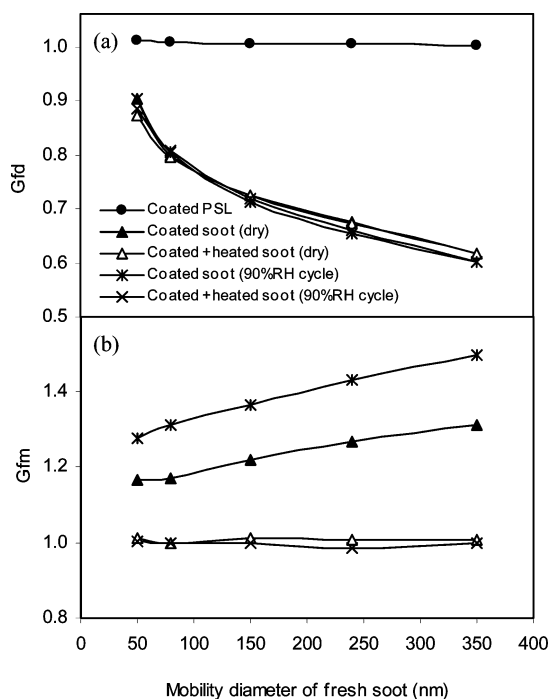


FIGURE 4. Mobility diameter (a) and mass (b) growth factors of soot and PSL particles upon coating by glutaric acid. Measurements were performed using mobility-classified aerosol with initial diameters of 50, 80, 150, 240, and 350 nm.

No further restructuring occurs when coated soot particles are cycled through elevated RH. After the acid is removed by heating, particle size does not recover to initial value and hence the restructuring is irreversible. The spherical PSL particles always show slightly increased mobility diameter upon condensation of glutaric acid.

Figure 4b illustrates changes in the particle mass upon coating of soot with glutaric acid as a function of initial mobility diameter. The mass growth factors vary between 1.17 and 1.31, which corresponds to a 14–24% glutaric acid fraction of the coated particle mass. Heating the coated particles completely removes glutaric acid (mass growth factor 1.00 ± 0.05), in agreement with the results of a fast flow reactor study (17) that reported a reversible uptake of glutaric acid on propane soot.

Mass growth factor of glutaric acid-coated soot increases with the initial particle size (Figure 4b), in contrast to the trend observed for succinic acid-coated soot (Figure 2b). Also, when soot aerosol is subjected to a lower concentration of glutaric acid vapor (8×10^{11} molecule cm^{-3}), the aggregates

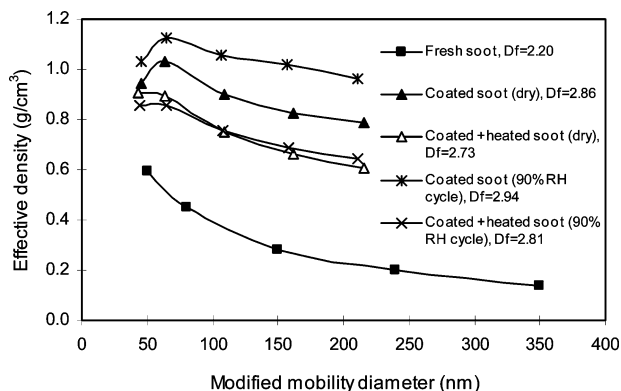


FIGURE 5. Effective densities of fresh and glutaric acid-coated soot as a function of processed mobility diameter.

shrink considerably, but only a small increase in the particle mass is detected. The striking inconsistency between changes in the coated particle size and mass is caused by partial evaporation of the glutaric acid coating during aerosol transport from the coating chamber to DMA2 and APM. Indeed, using TDMA measurements for pure glutaric acid aerosol, we observe a 11–45% mobility size decrease for particles of the initial sizes of 80–350 nm. Cruz et al. (18) also reported partial losses of pure glutaric acid from particles that led to uncertainties during aerosol deliquescence measurements.

The high RH cycle, while having a small effect on the mobility size, causes an unexpectedly significant increase in the mass of coated soot particles. Above the deliquescence RH (Table 1), water condenses on the coated particle surface, dissolving glutaric acid and increasing the coating volume. Upon drying to 5% RH, a small fraction of water remains trapped within the coating, leading to the observed mass increase. The particle mobility size remains practically constant because the additional coating volume occupies the external pseudovoid space (5) between the primary carbon spheres.

The effective density of soot particles increases significantly upon coating with glutaric acid, as shown in Figure 5. Coated and heated soot is 1.5–3.0 times denser than fresh soot. Since the mass of particles first coated and then heated is similar to that of fresh soot, the increased effective density of the soot cores is caused by restructuring to a more compact morphology. A significant additional increase in the effective density of coated particles occurs upon exposure to high RH cycle. A distinct maximum of effective density observed for the processed soot at 80 nm arises because the smallest coated particles ($d_{me} = 50$ nm) have the highest relative evaporation rate of the coating compared to the larger particles. A similar trend has been reported in previous studies for the density of diesel exhaust particles (19).

The increase in particle mass and decrease in mobility size upon coating with glutaric acid are accompanied by an increase of the mass fractal dimension from 2.20 for fresh soot to 2.86 for coated soot and subsequently to 2.94 for coated soot cycled through elevated RH. When the coating is removed by heating, the D_f values decrease to 2.73 and 2.81 for dry and high RH cycle conditions, respectively, remaining significantly higher than the D_f for fresh soot.

In the case of liquid coatings, such as sulfuric acid (8) and ozonolysis products of α -pinene (20), the force leading to compaction of agglomerates is the surface tension of the liquid that brings the primary particles into a closer configuration in order to minimize the surface of the liquid (21). Once the contact region between the solid surfaces is replaced by a contact of liquid to liquid, restructuring of the agglomerates occurs. The extent of restructuring induced by condensation depends on the liquid–solid interaction, i.e.,

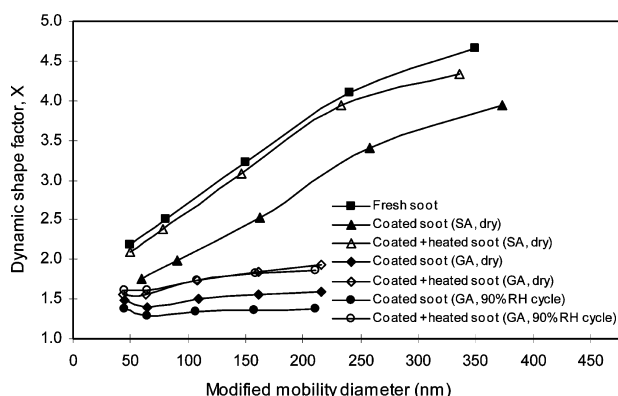


FIGURE 6. The dynamic shape factors as a function of mobility diameter for fresh and coated soot (SA = succinic acid, GA = glutaric acid).

surface tensions of the condensing liquid and the solid (22). For instance, significant restructuring has been observed for hydrophobic butane–air flame soot exposed to subsaturated vapors of n-hexane and 2-propanol whereas water vapor yielded nearly no effect (23). Slowik et al. (24) reported that liquid oleic acid coatings rearranged the soot aggregates to a more compact configuration whereas this rearrangement did not occur for solid anthracene coatings.

The restructuring mechanism described above appears to be inapplicable to glutaric acid, as it is present in a crystalline state at room temperature under dry conditions. To rationalize why glutaric acid promotes restructuring of soot aggregates in contrast to succinic acid, one needs to consider that glutaric acid has a significantly lower melting temperature than that of succinic acid (Table 1). The lower melting temperature of glutaric acid is caused by the twisted molecular conformation in the crystal lattice due to the presence of an odd number of carbon atoms in its molecule. Indeed, melting points of dicarboxylic acids show an alternating trend where the acids containing even number of carbon atoms exhibit systematically higher melting points compared to odd ones (13). A similar trend has also been observed for vapor pressures and sublimation enthalpies, where higher pressures and lower enthalpies correspond to a less stable crystal structure of odd members (12). Strained torsional conformation of glutaric acid in the solid state and the associated excess energy as compared to succinic acid may lead to stronger interaction of glutaric acid with the soot surface. Because of this interaction, formation of a “subcooled” liquid rather than crystalline layer may be more thermodynamically or kinetically feasible when the first few monolayers of glutaric acid condense on the soot surface. This quasiliquid layer can promote the aggregate to collapse even under dry conditions as observed in the present study and reported earlier by Mikhailov et al. (7). Another indication of a strong interaction between glutaric acid and soot comes from our recent heterogeneous uptake study where desorption of glutaric acid (17) from the soot surface was found to be significantly slower than desorption of succinic acid (unpublished data).

Inherent Material Density and Dynamic Shape Factor.

For aggregates, even after coating and restructuring, the measured effective density is typically significantly lower than the inherent (true) material density. To estimate the inherent material density of coated soot, the mass fractions of soot, f_{soot} , and acid coating, f_{acid} , are determined from APM measurements. Using the inherent material densities of pure soot ($\rho_{\text{soot}} = 1.77 \text{ g cm}^{-3}$ (25)) and coating materials, ρ_{acid} (Table 1), the inherent material density of the coated soot particles ($\rho_{\text{coated, inherent}}$) is expressed as:

$$\rho_{\text{coated, inherent}} = \frac{1}{f_{\text{acid}}/\rho_{\text{acid}} + f_{\text{soot}}/\rho_{\text{soot}}} \quad (4)$$

The calculated values of inherent material densities, $1.64\text{--}1.71 \text{ g cm}^{-3}$, are significantly higher than the measured effective densities (Figures 3 and 5), suggesting incomplete restructuring and the existence of the pseudovoids in the compacted soot (5).

On the basis of the inherent material density, the volume equivalent diameter (d_{ve}) can be determined, which is defined as the diameter of a spherical particle of the same volume as the irregularly shaped particle. The volume equivalent diameter is used to calculate the dynamic shape factor, χ , which is a measure of the increased drag experienced by an irregular particle in comparison to a sphere of equivalent volume moving at the same speed. The general expression for the dynamic shape factor is

$$\chi = \frac{d_{\text{me}}}{d_{\text{ve}}} \times \frac{C_{\text{ve}}}{C_{\text{me}}} \quad (5)$$

where C_{ve} and C_{me} are the Cunningham slip correction factors calculated for d_{ve} and d_{me} , respectively. The dynamic shape factor is always greater than unity for irregular particles and equal to unity for spheres.

Figure 6 compares the size-dependent dynamic shape factors for fresh soot with those for soot processed by condensation of succinic and glutaric acids. For fresh soot, χ increases from 2.2 to 4.7 with particle mobility diameter increasing from 50 to 350 nm. The dynamic shape factor of fresh soot is higher than that measured for diesel soot (26). Coating of the soot aggregates with organic acids lowers χ to 1.5–1.8 because the condensed material fills up the irregularities, reducing the drag. The dynamic shape factors of soot particles coated by glutaric acid are significantly lower than those for soot coated by succinic acid, in agreement with our fractal dimension analysis. For soot coated with glutaric acid, the dynamic shape factor decreases to 1.29–1.38 after exposure to high RH cycle. When the condensed glutaric acid is removed by heating, χ increases insignificantly, indicating a substantial restructuring of the soot cores. However, heating the soot coated with succinic acid restores χ to a value close to that measured for fresh soot because no restructuring occurs.

Atmospheric Implications. Our measurements show that the physical properties of dicarboxylic acids need to be taken into account when considering the internal mixing of these acids with soot. Exposure of soot aerosol to glutaric acid (C5) significantly increases the effective density and fractal dimension of the soot cores, whereas condensation of succinic acid (C4) does not promote the restructuring. Although soot aerosol may acquire a significant fraction of dicarboxylic acid coating during atmospheric aging, the extent of restructuring will strongly depend not only on the mass fraction but also on the type of acid. At elevated relative humidity, soot with highly soluble coating can experience additional compaction.

Hygroscopic particles produced through internal mixing of soot with glutaric acid deliquesce at subsaturated RH conditions and hence can play a role in haze formation. Also, deliquesced particles exhibit stronger light scattering and absorption (7), resulting in visibility reduction and altered direct climate forcing (27). As pure glutaric acid particles readily activate to cloud droplets at supersaturations below 0.3% (28), soot coated with glutaric acid may affect cloud formation and force climate indirectly. Increased hydrophilicity of coated soot reduces its lifetime in the atmosphere because hydrophilic soot particles are effectively removed by wet scavenging. Also, the changes in hygroscopicity, morphology, and effective density of soot aerosol during

atmospheric aging likely modify its deposition in human respiratory system and are hence relevant to health effects.

Further studies will need to include a wider (C3–C9) range of dicarboxylic acids to assess how the effect on soot restructuring varies with molecular size. Also, other organic species produced from oxidation of volatile organic compounds (29, 30), in addition to organic acids, can interact with soot either by condensation or via heterogeneous reactions (31, 32). The knowledge of the chemical composition of the coating materials is crucial when evaluating the optical and CCN properties of internally mixed soot aerosol.

Acknowledgments

This work was supported by the US Department of Energy National Institute for Climate Change Research (DOE-NICCR) and Robert A. Welch Foundation (A-1417). R.Z. acknowledges additional support from the National Natural Science Foundation of China Grant (40728006).

Literature Cited

- Jacobson, M. Z. Strong radiative heating due to the mixing state of black carbon in atmospheric aerosols. *Nature* **2001**, *409* (6821), 695–697.
- Li, G. H.; Zhang, R. Y.; Fan, J. W.; Tie, X. X. Impacts of black carbon aerosol on photolysis and ozone. *J. Geophys. Res.* **2005**, *110* (D23), D23206.
- Zhang, R.; Lei, W.; Tie, X.; Hess, P. Industrial emissions cause extreme diurnal urban ozone variability. *Proc. Natl. Acad. Sci. U.S.A.* **2004**, *101* (17), 6346–6350.
- Zhang, D.; Zhang, R. Laboratory investigation of heterogeneous interaction of sulfuric acid with soot. *Environ. Sci. Technol.* **2005**, *39* (15), 5722–5727.
- DeCarlo, P. F.; Slowik, J. G.; Worsnop, D. R.; Davidovits, P.; Jimenez, J. L. Particle morphology and density characterization by combined mobility and aerodynamic diameter measurements. Part I: Theory. *Aerosol Sci. Technol.* **2004**, *38* (12), 1185–1205.
- McMurry, P. H.; Wang, X.; Park, K.; Ehara, K. The relationship between mass and mobility for atmospheric particles: A new technique for measuring particle density. *Aerosol Sci. Technol.* **2002**, *36* (2), 227–238.
- Mikhailov, E. F.; Vlasenko, S. S.; Podgorny, I. A.; Ramanathan, V.; Corrigan, C. E. Optical properties of soot-water drop agglomerates: An experimental study. *J. Geophys. Res.* **2006**, *111* (D7), D07209.
- Zhang, R.; Khalizov, A. F.; Pagels, J.; Zhang, D.; Xue, H.; McMurry, P. H. Variability in morphology, hygroscopicity, and optical properties of soot aerosols during atmospheric processing. *Proc. Natl. Acad. Sci. U.S.A.* **2008**, *105* (30), 10291–10296.
- Weingartner, E.; Burtscher, H.; Baltensperger, U. Hygroscopic properties of carbon and diesel soot particles. *Atmos. Environ.* **1997**, *31* (15), 2311–2327.
- Park, K.; Cao, F.; Kittelson, D. B.; McMurry, P. H. Relationship between particle mass and mobility for diesel exhaust particles. *Environ. Sci. Technol.* **2003**, *37* (3), 577–583.
- Zhang, R.; Suh, I.; Zhao, J.; Zhang, D.; Fortner, E. C.; Tie, X.; Molina, L. T.; Molina, M. J. Atmospheric new particle formation enhanced by organic acids. *Science* **2004**, *304* (5676), 1487–1490.
- Bilde, M.; Svenningsson, B.; Monstern, J.; Rosenorn, T. Even-odd alternation of evaporation rates and vapor pressures of C3–C9 dicarboxylic acid aerosols. *Environ. Sci. Technol.* **2003**, *37* (7), 1371–1378.
- Thalladi, V. R.; Nüsse, M.; Boese, R. The melting point alternation in α,ω -alkanedicarboxylic acids. *J. Am. Chem. Soc.* **2000**, *122* (38), 9227–9236.
- Fortner, E. C.; Zhao, J.; Zhang, R. Y. Development of ion drift-chemical ionization mass spectrometry. *Anal. Chem.* **2004**, *76* (18), 5436–5440.
- Zhao, J.; Zhang, R.; Fortner, E. C.; North, S. W. Quantification of hydroxycarbonyls from OH-isoprene reactions. *J. Am. Chem. Soc.* **2004**, *126* (9), 2686–2687.
- Zhao, J.; Zhang, R. Proton transfer reaction rate constants between hydronium ion (H_3O^+) and volatile organic compounds (VOCs). *Atmos. Environ.* **2004**, *38* (14), 2177–2185.
- Levitt, N. P.; Zhang, R. Y.; Xue, H. X.; Chen, J. M. Heterogeneous chemistry of organic acids on soot surfaces. *J. Phys. Chem. A* **2007**, *111* (22), 4804–4814.
- Cruz, C. N.; Pandis, S. N. Deliquescence and hygroscopic growth of mixed inorganic-organic atmospheric aerosol. *Aerosol Sci. Technol.* **2000**, *34* (20), 4313–4319.
- Maricq, M. M.; Podsiadlik, D. H.; Chase, R. E. Size distributions of motor vehicle exhaust PM: A comparison between ELPI and SMPS measurements. *Aerosol Sci. Technol.* **2000**, *33* (3), 239–260.
- Saathoff, H.; Naumann, K. H.; Schnaiter, M.; Schöck, W.; Möhler, O.; Schürath, U.; Weingartner, E.; Gysel, M.; Baltensperger, U. Coating of soot and $(NH_4)_2SO_4$ particles by ozonolysis products of alpha-pinene. *J. Aerosol Sci.* **2003**, *34* (10), 1297–1321.
- Glasstetter, R.; Ricketts, C. I.; Wilhelm, J. G. Towards modeling the meniscus geometry and volume of capillary water between two contacting microspheres in moist air. *J. Aerosol Sci.* **1991**, *22* (Suppl. 1), S195–S198.
- Topping, D. O.; McFiggans, G. B.; Kiss, G.; Varga, Z.; Facchini, M. C.; Decesari, S.; Mircea, M. Surface tensions of multi-component mixed inorganic/organic aqueous systems of atmospheric significance: measurements, model predictions and importance for cloud activation predictions. *Atmos. Chem. Phys.* **2007**, *7* (9), 2371–2398.
- Kütz, S.; Schmidt-Ott, A. Characterization of agglomerates by condensation-induced restructuring. *J. Aerosol Sci.* **1992**, *23* (Suppl. 1), 357–360.
- Slowik, J. G.; Cross, E. S.; Han, J. H.; Kolucki, J.; Davidovits, P.; Williams, L. R.; Onasch, T. B.; Jayne, J. T.; Kolb, C. E.; Worsnop, D. R. Measurements of morphology changes of fractal soot particles using coating and denuding experiments: Implications for optical absorption and atmospheric lifetime. *Aerosol Sci. Technol.* **2007**, *41* (8), 734–750.
- Park, K.; Kittelson, D. B.; Zachariah, M. R.; McMurry, P. H. Measurement of inherent material density of nanoparticle agglomerates. *J. Nanopart. Res.* **2004**, *6* (2–3), 267–272.
- Park, K.; Kittelson, D. B.; McMurry, P. H. Structural properties of diesel exhaust particles measured by transmission electron microscopy (TEM): Relationships to particle mass and mobility. *Aerosol Sci. Technol.* **2004**, *38* (9), 881–889.
- Zhang, R. Y.; Li, G. H.; Fan, J. W.; Wu, D. L.; Molina, M. J. Intensification of Pacific storm track linked to Asian pollution. *Proc. Natl. Acad. Sci. U.S.A.* **2007**, *104* (13), 5295–5299.
- Prenni, A. J.; DeMott, P. J.; Kreidenweis, S. M.; Sherman, D. E.; Russell, L. M.; Ming, Y. The effects of low molecular weight dicarboxylic acids on cloud formation. *J. Phys. Chem. A* **2001**, *105* (50), 11240–11248.
- Suh, I.; Zhang, R.; Molina, L. T.; Molina, M. J. Oxidation mechanism of aromatic peroxy and bicyclic radicals from OH-toluene reactions. *J. Am. Chem. Soc.* **2003**, *125* (41), 12655–12665.
- Zhang, D.; Zhang, R.; Park, J.; North, S. W. Hydroxyperoxy nitrites and nitrates from OH initiated reactions of isoprene. *J. Am. Chem. Soc.* **2002**, *124* (32), 9600–9605.
- Zhao, J.; Levitt, N. P.; Zhang, R. Y. Heterogeneous chemistry of octanal and 2,4-hexadienal with sulfuric acid. *Geophys. Res. Lett.* **2005**, *32* (9), L09802.
- Zhao, J.; Levitt, N. P.; Zhang, R.; Chen, J. Heterogeneous reactions of methylglyoxal in acidic media: Implications for secondary organic aerosol formation. *Environ. Sci. Technol.* **2006**, *40* (24), 7682–7687.

ES803287V